Journal of Agricultural Sciences
(Tarim Bilimleri Dergisi)

J Agr Sci-Tarim Bili
e-ISSN: 2148-9297
jas.ankara.edu.tr

JAS

Characterization and antimicrobial properties of silver nanoparticules biosynthesized from cornelian cherry (*Cornus mas* L.)

Tuğçe Özeşer[a], Nural Karagozlu[a*]

[a]*Manisa Celal Bayar University, Engineering Faculty, Food Engineering Department, Manisa, TÜRKİYE*

ARTICLE INFO
Research Article
Corresponding Author: Nural Karagozlu, E-mail: nural.karagozlu@cbu.edu.tr
Received: 25 July 2023 / Revised: 18 November 2023 / Accepted: 10 January 2024 / Online: 23 July 2024

Cite this article
Özeşer T, Karagozlu N(2024). Characterization and antimicrobial properties of silver nanoparticules biosynthesized from cornelian cherry (*Cornus mas* L.). *Journal of Agricultural Sciences (Tarim Bilimleri Dergisi),* 30(3):444-457. DOI: 10.15832/ankutbd.1332427

ABSTRACT
Nanoparticles produced by green synthesis has been increasingly gaining popularity, especially because they are eco-friendly and low cost. In the present article, silver nanoparticles (AgNPs) were synthesized from the extracts prepared using cornelian cherry (*Cornus mas* L.) at two different temperatures. The properties of obtained AgNPs were determined through UV-Vis spectroscopy, SEM, EDX, FTIR, and XRD analyses, and their antimicrobial effects on four pathogenic bacteria were investigated. The analysis results conducted using UV-spectrophotometry, SEM, EDX, FTIR, and XRD on AgNPs prepared from extracts obtained at two different temperatures (20 °C and 60 °C) were similar. The groups playing a role in nanoparticle formation were determined to be C=C, C=O, and C-O, and it was also concluded that the two different extraction temperatures had no significant effect on nanoparticle synthesis and characterization. The cherry extract's antimicrobial activity was effective against *Staphylococcus aureus, Listeria monocytogenes, and Salmonella* Typhi, while it didn't show activity against *Escherichia coli* O157:H7. The AgNPs at concentration of 25 mg/mL created inhibition zones of 9 mm, 9 mm, and 7 mm for *L.monocytogenes*, *S.aureus*, and *S.*Typhi, respectively, at 20 °C. It was seen that 25 mg/mL AgNPs synthesized at 60 °C formed 9 mm and 8 mm inhibition zones in *S.aureus* and *L.monocytogenes* cultures, respectively, whereas they showed no inhibiting activity against *S.*Typhi, and *E.coli* O157:H7. It has been seen that 20 °C has ease of application in two different temperatures applied in the preparation of silver nanoparticles and is a good alternative to chemical methods.

Keywords: Silver nanoparticles, Antimicrobial effects, Cornelian cherry, *Cornus mas* L., Green synthesis

1. Introduction

Particles with sizes below 100 nm are referred to as nanoparticles, and metals whose sizes are reduced through various methods can acquire different properties (Rai & Bai 2011; Wang et al. 2011). Metal nanoparticles can be obtained through physical and chemical methods. Nevertheless, these methods possess drawbacks, including elevated costs, slow production rates, increased energy demands, and the potential of toxicity. Therefore, in recent years, a biological method called green synthesis has gained importance and has been used for nanoparticle synthesis. This method offers advantages over other methods, including low cost, rapid production, ease of acquisition, eco-friendliness, low energy requirements, non-toxicity of the resulting nanoparticles, biocompatibility, and ease of sustainability. Biological agents such as bacteria, yeast, fungi, algae, and plants are used as reducing and stabilizing agents in nanoparticle synthesis, and the synthesis is achieved through the reduction of metal salts facilitated by the metabolites they contain (Arshadi et al. 2018; Rezvani et al. 2019). During the synthesis of nanoparticles, various metabolites contained within plants play a crucial role in the reduction of silver ions. Vitamins, proteins, amino acids, and polysaccharides found in these plants facilitate the formation of nanoparticles, while alkaloids, terpenes, glycosides, and flavonoids are involved in the reduction of silver ions and the stability of nanoparticles (Arya et al. 2019; Paiva-Santos et al. 2021). The primary component responsible for nanoparticle formation, as reported by Ceylan et al. (2021) in their study with three *Sideritis* species, is chlorogenic acid, whereas Ekrikaya et al. (2021), in their research with berries, identified ellagic acid as the key compound. The synthesis process is rooted in the reduction of metal salts using plant extracts. Various factors such as synthesis time, pH, reaction temperature and duration, metal type and concentration, and extract-to-metal salt ratio affect the characteristics of nanoparticles, such as size and shape (Arya et al. 2019; Rana et al. 2020; Alkhattaf 2021; Paiva-Santos et al. 2021).

The use of silver in nanoparticle synthesis has increased compared to other metals due to its lower toxicity and antimicrobial effects, leading to extensive research in the fields of food and healthcare (Silver 2003; Rai et al. 2011). Silver nanoparticles (AgNPs) are known for their optical, catalytic, and electrical properties, in addition to their remarkable oxidative resistance, high stability, surface reactivity, and the ease with which their surfaces can be modified (Paiva-Santos et al. 2021). Furthermore, the antimicrobial activity of AgNPs is noteworthy. AgNPs weaken the cell wall through electrostatic interactions, enter the bacterial

cell, inhibit bacterial growth, and cause cell death. Several studies have been conducted to illustrate the electrostatic attraction between positively charged nanoparticles (NPs) and negatively charged bacterial cells. These NPs have been observed to accumulate within the cell membrane, potentially penetrating and causing damage to the cell wall or membrane. It is hypothesized that silver ions bind to thiol groups (-SH) and subsequently induce deactivation within the cell membrane. Furthermore, it is suggested that silver ions may denature the DNA molecule by disrupting the hydrogen bonds between the two strands of DNA and intercalating between purine and pyrimidine base pairs. Factors including nanoparticle size, shape, surface charge, nanoparticle concentration, bacterial species, and the bacterial counts impact antimicrobial activity (Cao et al. 2001; Ghaedi et al. 2015; Abbasi et al. 2016; Arya et al. 2019; Hernandez Morales et al. 2019).

Nanotechnology as a packaging material in food production has gained importance in reducing energy consumption, improving gas barrier properties, and reducing CO_2 emissions to preserve human and environmental health (Baysal 2020). With the increasing interest of consumers in healthier, minimally processed, additive-free food products, producers have started to utilize nanotechnology to meet these demands by extending the shelf life of food, preserving food nutritional values, and developing new products. A study indicated that using AgNPs in fruit storage can extend the shelf life by catalyzing the ethylene gas and slowing respiration (Polat & Fenercioğlu 2014).

It has also been shown that nanoparticles could find applications in the fields of food and healthcare, thanks to their low toxicity and antimicrobial properties. (Ceylan et al. 2021). The application areas of AgNPs in the food industry include food packaging materials, ensuring food safety, and water disinfection. However, with the growing interest in AgNPs synthesized through biological methods, research is also being conducted on improving the texture and aroma properties of food, extending the shelf life of food, and preserving food nutritional values (Sürengil & Kılınç 2011).

In this study, silver nanoparticles (AgNPs) were synthesized using cornelian cherry (*Cornus mas* L.), a shrub-like plant belonging to the *Cornaceae* family of the *Umbelliflorae* order, which grows in Central and Southeastern Europe, including Ukraine, Georgia, Armenia, the Czech Republic, Slovakia, Turkey, Serbia, Austria, and Poland. Cornelian cherry is a red oval-shaped fruit with different species. Cornelian cherry is one of the fruits that naturally grow in Turkey and it has been used in folk medicine for centuries mainly in Anatolia to prevent some diseases (Celep et al. 2012). It contains phenolic compounds, mineral substances, vitamin C, anthocyanins, flavonoids, and polyphenols. It also exhibits antioxidant and anti-inflammatory properties (Stankovic et al. 2014; Salejda et al. 2018). Cornelian cherry (*Cornus mas* L.) fruit, naturally growing in Anatolia, was selected for this study owing to its economic significance and its observed antimicrobial properties. In contemporary times, silver, a historical agent for infection control and preservation, has garnered attention as it has not been synthesized in cranberries to date. It was aimed to determine the basic properties of AgNPs synthesized from extracts obtained from *Cornus mas* L. fruit at two different extraction temperatures, which have yet to be used in previous studies. The antimicrobial activity of the obtained AgNPs against some foodborne pathogenic bacteria, including *Staphylococcus aureus, Listeria monocytogenes, Salmonella* Typhi, and *Escherichia coli* O157:H7, was also investigated. For this purpose, the properties of AgNPs obtained from extracts prepared at two different temperatures, 20 °C and 60 °C, were determined using UV-Vis spectrophotometry, FTIR, EDX, XRD, and SEM, and their antimicrobial properties were investigated using the paper disc method on some foodborne pathogenic bacteria.

2. Material and Methods

2.1. Materials

The cornelian cherry fruit (*Cornus mas* L.) used in the study was freshly obtained from a local market in August. The cherries were washed, deseeded, dried in a rotary tray dryer at 65 °C, and grinded. The dried cherries were stored in glass jars in a cool and dark environment until further use.

2.2. Method

2.2.1. Preparation of cornelian cherry extract

Room temperatures (20 °C) and 60 °C were applied to prepare the cornelian cherry extract. 10 g of dried cherries were mixed with 100 mL of distilled water. The mixture was agitated in an orbital shaker at 135 rpm for 30 minutes and then kept in a dark environment for 24 hours. The obtained cornelian cherry extract was filtered through Whatman No.1 filter paper and centrifuged at 4100 rpm for 15 minutes (NÜVE NF 800R). The supernatant was collected to obtain the extract for further use (Figures 1 and 2).

Figure 1- (a) Cornelian cherry extract prepared at 20 °C, (b) extract after 24 hours, (c) filtered extract

Figure 2- (a) Cornelian cherry extract prepared at 60 °C, (b) extract after 24 hours, (c) filtered extract

2.2.2. Silver nanoparticle synthesis

For the synthesis of AgNPs, 10 mL of cornelian cherry (*Cornus mas* L.) extract was mixed with 90 mL of 1 mM $AgNO_3$ (Carlo Erba, 423952) solution and agitated in a shaker incubator at room temperature, 135 rpm, for 90 minutes, in a light-protected environment. Subsequently, it was kept in a dark environment for 24 hours, and color change was observed (Figure 3 and Figure 4). Spectrum analysis was performed using UV spectroscopy.

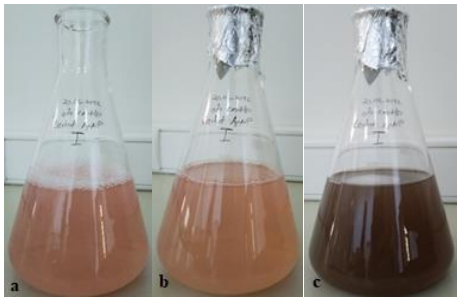

Figure 3- AgNP solution obtained from cornelian cherry extract prepared at 20 °C (a) 0 min, (b) 90 min, (c) 24 hours

Figure 4- AgNP solution obtained from cornelian cherry extract prepared at 60 °C (a) 0 min, (b) 90 min, (c) 24 hours

For the purification of AgNPs, centrifugation was performed at 4100 rpm for 25 minutes, and the supernatant was discarded. The precipitate was washed several times by adding distilled water. After this process, the AgNPs were transferred to Petri dishes, dried in a vacuum oven at 65 °C, and stored in a dark environment at room conditions (Figure 5).

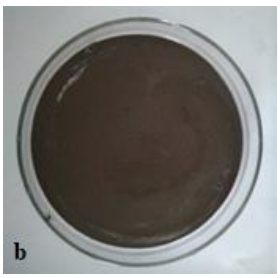

Figure 5- Cornelian cherry AgNPs after drying

2.2.3. Characterization of synthesized silver nanoparticles

The spectrophotometric analysis of the extract and nanoparticles was performed using a Shimadzu UV-1601 UV-Vis spectrophotometer in the wavelength range of 200-1000 nm. Spectrum acquisition was conducted against pure water at a medium speed.

Scanning Electron Microscopy (SEM) to determine the morphological structure of AgNPs while Energy-Dispersive X-ray Spectroscopy (EDX) was utilized to confirm the presence of silver (ZEISS GeminiSEM 500). Carbon tape was used in the SEM analysis, and the gold coating was applied under a vacuum to ensure the conductivity of the nanoparticles. ImageJ software determined particle size, and a histogram graph was plotted using the Statistical Package for the Social Sciences (SPSS) program.

Fourier Transform Infrared Spectroscopy (FTIR, Thermo Scientific Nicolet IS20) analysis was performed in the range of 4000-400 cm^{-1} to determine the functional groups responsible for the reduction in the extracts and involved in AgNP synthesis.

X-Ray Diffraction (XRD) analyses were carried out in the PANalytical EMPYREAN instrument in the range of $5° \leq 2\theta \geq 85°$ to determine the crystal structure and size of AgNPs. The Debye-Scherrer equation, $D = K \lambda / (\beta \cos \theta)$, was used to calculate the particle size, where D represents the particle size (nm), K is a constant value (0.9), λ is the X-ray wavelength (Å) (1.54060), β is the half-width at the maximum peak value (FWHM) (rad), and θ is the angle of the maximum peak height (rad).

2.2.4. Determination of antimicrobial properties of synthesized silver nanoparticles

For the evaluation of the antimicrobial properties of AgNPs synthesized from cornelian cherry (*Cornus mas* L.) through green synthesis, *Staphylococcus aureus* (ATCC 12600), *Listeria monocytogenes* (ATCC 7644), *Salmonella* Typhi (ATCC 14028), and *Escherichia coli* O157:H7 (ATCC 25922) bacteria were used. The cultures were obtained from the Department of Dairy Technology, Faculty of Agriculture, Ege University. The cultures were activated in 10 mL of Tryptic Soy Broth (Merck, 105459) and incubated at 37 °C for 24 hours. From this culture, 0.1 mL was transferred to a Petri dish, and approximately 15 mL of Tryptic Soy Agar (TSA, Merck, 105458) was added to prepare the medium for antimicrobial testing.

AgNPs were prepared at 10 and 25 mg/mL concentrations, and their antimicrobial activity was determined using the paper disk method. The nanoparticle solution was prepared using sterile distilled water and allowed to stand in an ultrasonic water bath for 1 hour for a homogeneous distribution. The AgNP solution was impregnated onto filter paper disks (Whatman No.1) and placed on the agar plates. A chloramphenicol antibiotic disk (Bioanalyse, 30 µg) was used for the positive control, and the extract concentration was prepared at a 1:1 ratio for the negative control.

2.2.5. Statistical analysis

The study was conducted in two parallel sets with three replicates each. The obtained microbiological analysis results were analyzed using the MANOVA (Multivariate Analysis of Variance) test in the SPSS program, and values below $p<0.05$ were considered statistically significant.

3. Results and Discussion

3.1. Determination of Properties of Silver Nanoparticles Obtained from Cornelian Cherry Extract

The properties of the AgNPs were determined through UV spectroscopy, SEM, EDX, FTIR, and XRD analyses. The silver nanoparticles (AgNPs) were obtained through biological synthesis using cornelian cherry (*Cornus mas* L.) extract at two different temperatures, 20 °C, and 60 °C. A color change from pink to brown was observed in nanoparticle synthesis at both temperatures, and the synthesis started after 24 hours.

The visible color change is the initial indicator that the biological synthesis of nanoparticles has begun. The synthesis time of nanoparticles depends on the pH of the environment. When the pH is low (acidic environment), the reaction starts later, and

the synthesis time can be longer (Alkhattaf 2021). Due to the pH value of 3 in the cornelian cherry extract, the color change occurred after 24 hours and shifted from pink to brown.

The spectrum analysis results of the extracts prepared at 20 °C and 60 °C revealed maximum absorbance peaks at 510 nm and 512 nm, respectively. The spectrum results of the AgNP solution derived from these extracts yielded the maximum peaks for the both temperatures at 500 nm (Figure 6 and Figure 7).

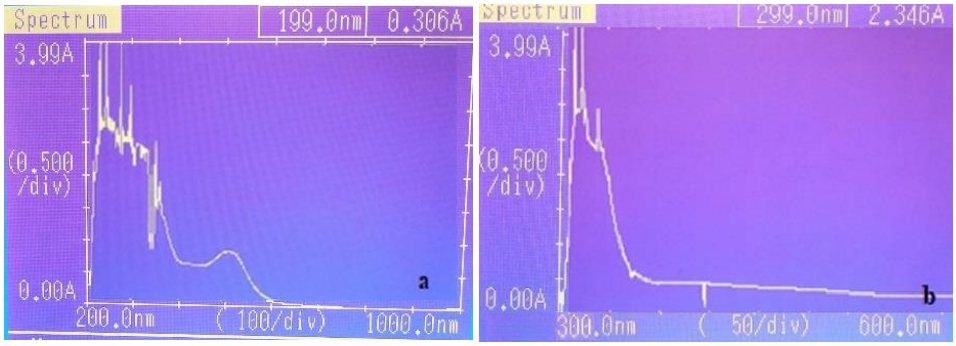

Figure 6- Spectrum graph of (a) cornelian cherry extract and (b) cornelian cherry AgNP solution prepared at 20 °C

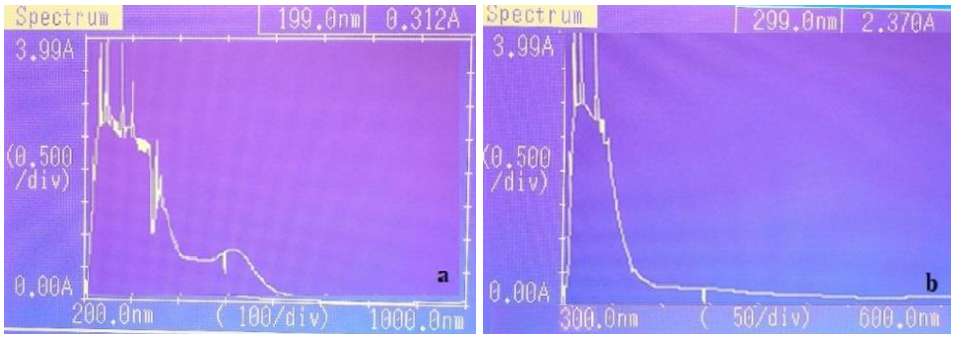

Figure 7- Spectrum graph of (a) cornelian cherry extract and (b) cornelian cherry AgNP solution prepared at 60 °C

In a study using *Cornus sanguinea* fruit similar to cornelian cherry, AgNPs obtained at room temperature showed a maximum absorbance peak at 510 nm (David et al. 2020). In this study, the result obtained at 20 °C was similar to our study; The temperature application of 60 °C showed a minor difference in the peak. In another cornelian cherry study, the maximum absorbance peak was observed at 418 nm (Filip et al. 2019). AgNPs derived from *Mangifera indica* fruit exhibited a maximum absorbance peak at 450 nm (Ameen et al. 2019). In a different study, *Rosa canina* fruit extract was obtained by heating for 5 minutes, and nanoparticles synthesized at 85 °C showed a maximum absorbance peak at 422 nm (Gulbagca et al. 2019). *Citrus sinensis* peels were used to synthesize AgNPs, and nanoparticle synthesis was carried out at two different temperatures, 25 °C and 60 °C, after boiling the extract in pure water for 2 minutes. The resulting nanoparticles exhibited maximum absorbance peaks at 445 nm for 25 °C and 424 nm for 60 °C, according to spectrophotometric analysis (Kaviya et al. 2011). As can be seen from the studies, the difference in fruit variety causes the change of the peaks.

In the morphology of nanoparticles, SEM analyses are used quite effectively for the size and shape of the nanomaterial (Ghaedi et al. 2015). SEM analysis of the AgNPs obtained from cornelian cherry extract at 20 °C and 60 °C. The SEM results and histogram graphs are presented in Figure 8 and Figure 9, respectively. The average sizes of AgNPs synthesized from the extracts at 20 °C and 60 °C were determined to be 50.86 nm and 61.17 nm, respectively. The AgNPs obtained at both temperatures exhibited spherical shapes.

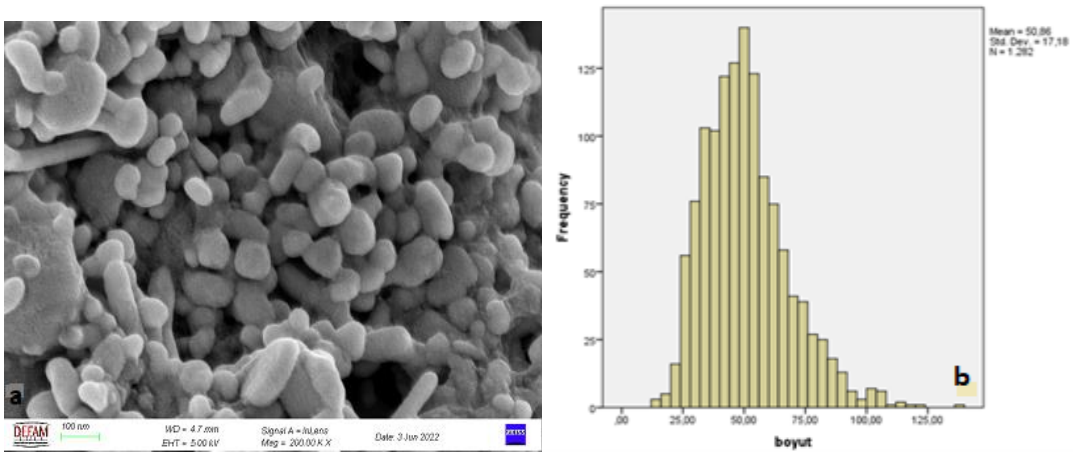

Figure 8- SEM results of nanoparticles obtained from the extract at 20 °C: (a) 200.00 K X, (b) histogram graph of nanoparticle size

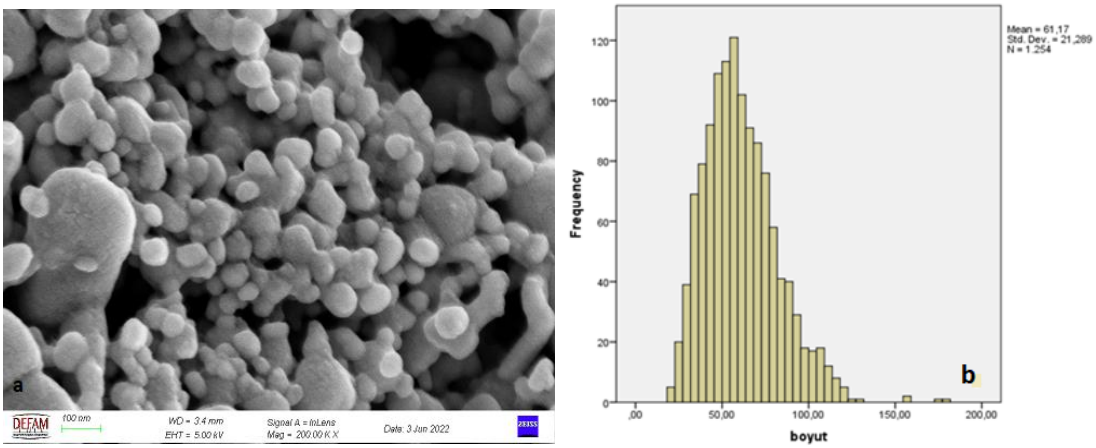

Figure 9- SEM results of nanoparticles obtained from the extract at 60 °C: (a) 200.00 K X, (b) histogram graph of nanoparticle size

The particle sizes of nanoparticles obtained from *Passiflora Edulis f. flavicarpa* leaves were reported to be between 50-100 nm, and their shapes were spherical in SEM and TEM analyses (Thomas et al. 2019). In the SEM analysis of AgNPs synthesized from Vitis vinifera, the particle sizes were reported to be between 30-70 nm, while in the TEM analysis, the sizes were found to be between 30-65 nm, and the shapes varied, including oval, triangular, and circular shapes (Hashim et al. 2020). In a study using *Berberis vulgaris* leaves and roots, the synthesized AgNPs were reported to have spherical shapes between 30-70 nm sizes in TEM analysis (Behravan et al. 2019). In TEM analysis, green-synthesized nanoparticles from Andean blackberry were reported to have spherical shapes and sizes between 12-50 nm (Kumar et al. 2017a).

Hernandez-Pinero et al. (2016) investigated the effects of different temperatures on the synthesis of AgNPs using basil, mint, marjoram, and peppermint. They observed that temperature had a significant impact on the synthesis process. They noted that varying heating rates resulted in AgNPs of different sizes, with higher heating rates leading to smaller AgNPs. In contrast, our study found that AgNPs synthesized at 60 °C were larger than those synthesized at 20 °C. However, as Hernandez-Pinero et al. (2016) pointed out, the choice of botanical species also influences the size of the AgNPs obtained. Therefore, it is possible to design a controlled system for synthesizing AgNPs with a specific diameter range by selecting particular plant species and heating rates to achieve nanoparticles of the desired size.

The scanning electron microscopy (SEM) images of the synthesized AgNPs reveal their length and homogeneity. These images indicate that the nanomaterials are spherical and of very small size. Due to their diminutive size, AgNPs can bind to cell membrane proteins and catalyze the generation of reactive oxygen species during bacterial growth, resulting in cell death due to oxidative stress (Alkhalaf et al. 2020). Consequently, the synthesized nanoparticles exhibited enhanced antimicrobial activity (Ramkumar et al. 2017; Lopes & Courrol 2018; Pallela et al. 2018).

EDX analysis was conducted to determine the elemental composition of AgNPs obtained from cornelian cherry extract at 20 °C and 60 °C. The findings of the EDX analysis are presented in Figure 3.5 and Figure 3.6. In the EDX results of the nanoparticles, strong peaks corresponding to silver at 3 eV were observed, confirming the formation of AgNP along with some weak peaks believed to originate from the fruit extract. The elemental composition of AgNPs synthesized after cornelian cherry

extraction at 20 °C was 82.82% Ag, 7.23% C, 1.40% O, and 8.55% Cl (Figure 10). The elemental composition of AgNPs obtained after extraction at 60 °C was determined as 83.64% Ag, 5.87% C, 1.26% O, and 9.24% Cl (Figure 11).

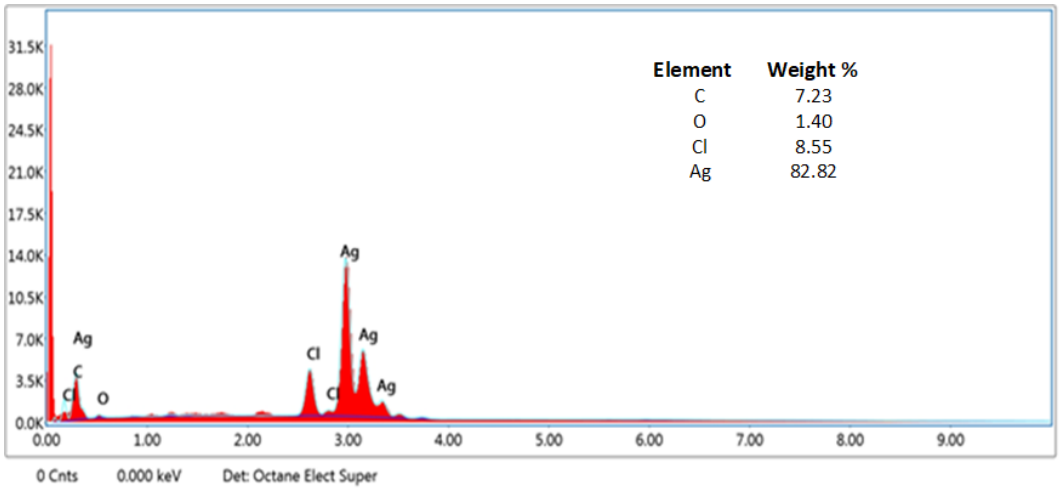

Figure 10- EDX result of the nanoparticles obtained from cornelian cherry extract at 20 °C

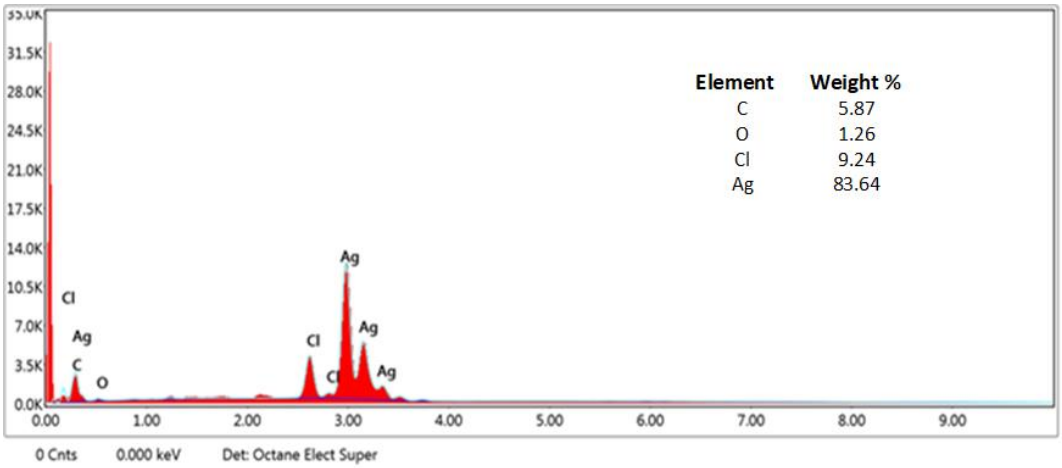

Figure 11- EDX result of the nanoparticles obtained from cornelian cherry extract at 60 °C

In the analysis using EDX, it was reported that nanoparticles obtained from garlic contained 75% Ag (Vijayakumar et al. 2019), nanoparticles obtained from *Mimusops elengi* fruit contained 47.6% Ag, 25.4% O, and 16.1% C (Korkmaz et al. 2020). AgNPs synthesized using *citrus sinensis* peels, *Capsicum annuum*, *Mespilus germanica* fruit, and *Prunus japonica* leaves were reported to exhibit strong silver peaks (Kaviya et al. 2011; Saravanakumar et al. 2017; Baran et al. 2020; Diler & Leblebicier 2020). In our study, the silver content of AgNPs obtained from both temperatures was relatively high.

Since the biological materials used in the synthesis of nanoparticles differ, each nanoparticle contains different components and functional groups, making it easier to determine the groups involved in reducing silver. FTIR analysis was conducted to identify the functional groups surrounding the nanoparticles and to determine the stabilizers (surface coatings) and reducing agents (Paiva-Santos et al. 2021).

The FTIR analysis results of cornelian cherry extract obtained at room temperature and the corresponding AgNPs are shown in Figure 12 and Figure 13. Regarding the peaks of the cornelian cherry obtained at 20 °C, the 2942 and 2884 cm^{-1} peaks were determined to be the C-H group (methyl, methylene and methoxy groups), the1731 cm^{-1} peak as the C=O group (aldehyde), the 1585 cm^{-1} peak as the C=O group (carboxyl group), 1346 cm^{-1} peak as the N=O group, the 1245 cm^{-1} peak as the C-O group and the 1072 cm^{-1} peak as the C=C group (aromatic ring). The spectrum peaks of AgNPs were determined to be 2113 cm^{-1}, 1988 cm^{-1}, 1503 cm^{-1} and 1274 cm^{-1}. The comparison of cornelian cherry extract and AgNPs suggested that C=O and C-O groups are involved in the reduction of silver.

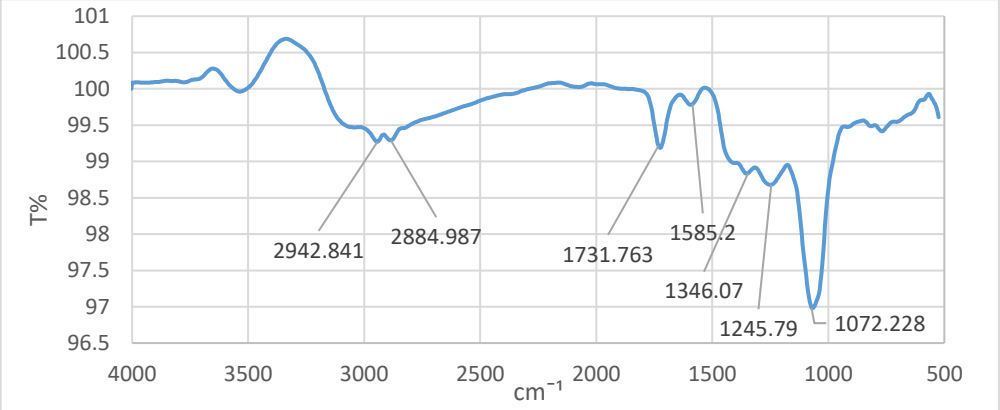

Figure 12- FTIR spectrum of the cornelian cherry extract obtained at 20 °C

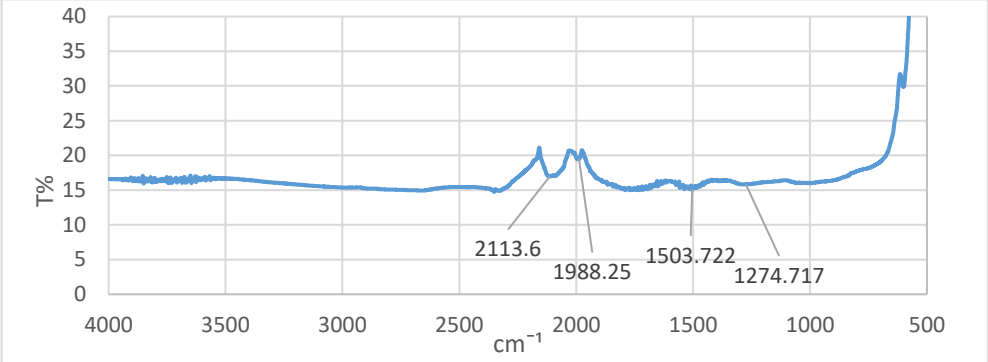

Figure 13- FTIR spectrum of the silver nanoparticles (AgNPs) obtained from cornelian cherry extract at 20 °C

The FTIR analysis results of cornelian cherry extract prepared by extraction at 60 °C and AgNP obtained from this extract are presented in Figures 14 and 15. In the FTIR spectrum of cornelian cherry extract obtained at 60 °C, the peak values correspond to 2917 and 2848 cm^{-1} for the C-H group, 1724 cm^{-1} for C=O, 1591 cm^{-1} for C=O group, 1343 cm^{-1} for N=O group, 1236 cm^{-1} for C-O group, and 1083 cm^{-1} for C=C groups. The spectrum peaks formed by AgNPs were observed at 2107 cm^{-1}, 1985 cm^{-1}, 1536 cm^{-1}, and 1046 cm^{-1}, and, comparing the spectrum peaks of *Cornus mas* L. extract with AgNPs, it was thought that the C=O and C=C groups play a role in reducing silver and contributing to AgNP formation.

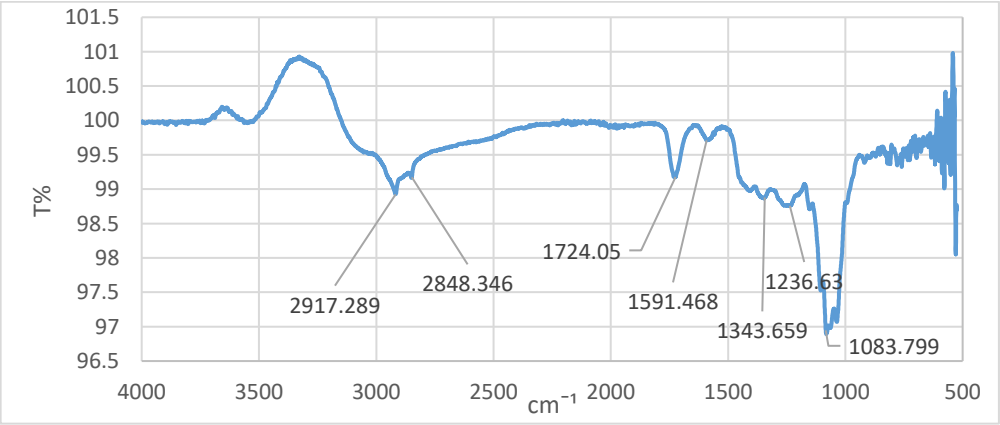

Figure 14- FTIR spectrum of the cornelian cherry extract obtained at 60 °C

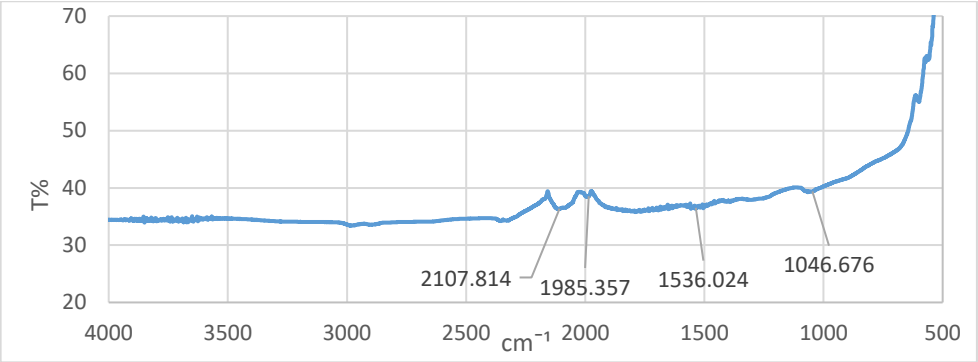

Figure 15- FTIR spectrum of the silver nanoparticles (AgNPs) obtained from cornelian cherry extract at 60 °C

The absorbance peaks of the extract and nanoparticle of silver nanoparticles synthesized using Cornus sanguinea fruit leaves were determined to be 3392-3434 cm^{-1} (O-H) and 1594-1618 cm^{-1} (C=O), indicating the presence of groups involved in Ag reduction (David et al. 2020). The FTIR analysis of the extract and synthesized AgNPs from Cornus officinalis fruit revealed peaks at 3352 and 3371 cm^{-1} (O-H), 2984 and 2983 cm^{-1} (C-H), 1655 and 1651 cm^{-1} (C=O), 1450 and 1448 cm^{-1}, 1273 and 1275 cm^{-1}, 1045 and 1049 cm^{-1} (C=C), indicating the presence of groups involved in Ag reduction (He et al. 2017). The extract derived from Prunus japonica exhibited peaks at 3284 cm^{-1} (N-H), 2927 cm^{-1} (C-H), 2363 cm^{-1} (C-H), 1598 cm^{-1} (C=O), 1384 cm^{-1} (alcohol, ethers, esters, carboxylic acids, and amino acids), and 1070 cm^{-1} (C-OH). A comparison of the peak values of the synthesized AgNPs from this extract revealed the involvement of C=O, N-H, and C-H groups in reduction (Saravanakumar et al. 2017). The peaks of AgNPs obtained from Mangifera indica extract were found to be at 3734 cm^{-1} (O-H), 2950 cm^{-1} (-CH), 2350 cm^{-1} (C-H), 1530 cm^{-1} (C-O), and 1030 cm^{-1} (N-O), indicating the involvement of these compounds in Ag reduction (Ameen et al. 2019). In the FTIR analysis of nanoparticles obtained from blackberry have been reported to be 3275 cm^{-1} (O-H) and 1634 cm^{-1} (C=O) groups, responsible for Ag reduction (Kumar et al. 2017a). The FTIR analysis of nanoparticles synthesized from cornelian cherry extract reported that the responsible groups for Ag reduction were 3159 cm^{-1} (O-H), 1717 cm^{-1} (C=O), and 1224 cm^{-1} (C-OO) (Filip et al. 2019).

Based on our results, the FTIR spectra obtained for both temperature applications were similar, and the groups involved in the reduction of silver and the formation of nanoparticles from cornelian cherry extract were determined to be C=C, C=O, and C-O (Figure 12, Figure 13, Figure 14, and Figure 15). These groups play a role as secondary metabolites in Ag reduction and the stability of nanoparticle formation (Arya et al. 2019; Paiva-Santos et al. 2021). Compared with previous studies, our results indicated the presence of similar groups of phytochemicals involved in Ag reduction.

The determination of the crystal structure and size of nanoparticles is provided by X-ray diffraction (XRD) analysis, which allows the identification of atom types through the diffraction of X-rays (Rana et al. 2020). In this context, XRD analysis was performed to determine the crystal structure and size of silver nanoparticles synthesized from cornelian cherry extract at 20 °C.

The average crystal sizes of AgNPs synthesized from the extract obtained at 20 °C were determined to be 38.81 nm using the Debye-Scherrer equation, and their nanoparticle structures were found to be face-centered cubic. The peak points at 2θ angles were determined as 38.22°, 44.41°, 64.57°, 77.49°, and 81.61°, corresponding to the Bragg diffraction planes of (111), (200), (220), (311), and (222), respectively (Figure 16).

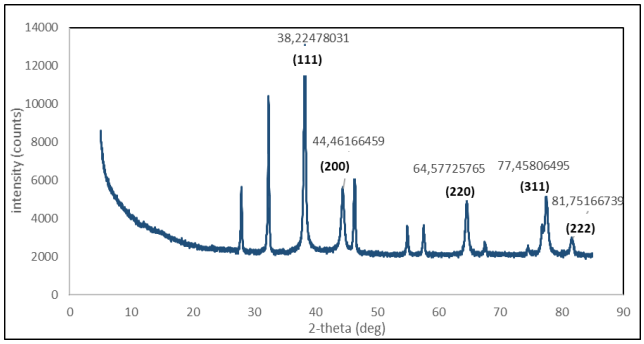

Figure 16- XRD result of AgNPs synthesized from cornelian cherry extract at 20 °C

The average crystal sizes of AgNPs synthesized from the extract obtained at 60 °C were found to be 37.88 nm, and their nanoparticle structures were determined to be face-centered cubic. The peak points at 2θ angles were determined as 38.12°, 44.34°, 64.44°, 77.38°, and 81.52°, corresponding to the diffraction planes of (111), (200), (220), (311), and (222), respectively (Figure 17).

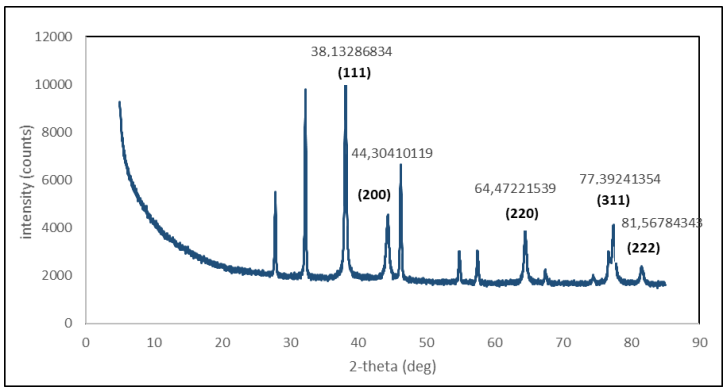

Figure 17- XRD result of AgNPs synthesized from cornelian cherry extract at 60 °C

The diffractions of AgNPs synthesized from *Rosa canina* were reported to be (111), (200), (220), (311), and (222), with a crystal size of 19.75 nm and a cubic crystal structure (Gulbagca et al. 2019). AgNPs synthesized from *Prunus persica* leaves showed diffractions of (111), (200), (220), (311), and (222), with a crystal size of 40 nm (Kumar et al. 2017b). AgNPs synthesized from *Mimusops elengi* exhibited 2θ values of 32.56°, 38.45°, 44.69°, 64.86°, 81.77°, and an average crystal size of 43 nm (Korkmaz et al. 2020). AgNPs synthesized from *Berberis vulgaris* leaves, and roots were determined to have crystal sizes of 50 nm (Behravan et al. 2019). AgNPs synthesized from apple showed 2θ values of 38.15°, 44.35°, 64.59°, 77.47°, 81.60°, corresponding diffractions of (111), (200), (220), (311), (222), and an average crystal size of 30 nm, with a cubic crystal structure [Ali et al. 2016]. AgNPs synthesized from *Forsythia suspensa* exhibited 2θ values of 38.23°, 46.31°, 64.58°, 77.50°, corresponding diffractions of (111), (200), (220), (311), and an average crystal size of 47.3 nm (Du et al. 2019).

In the present study, the crystal sizes of the nanoparticles synthesized from the extracts obtained at 20 °C and 60 °C were calculated as 38.81 nm and 37.88 nm, respectively (Figure 3.11 and Figure 3.12). It was determined that the shapes of the nanoparticles were cubic crystals for both temperature values. When compared with the SEM results, the average sizes of the nanoparticles synthesized from the extracts obtained at 20 °C and 60 °C were calculated as 50.86 nm and 61.17 nm, respectively, and these values were close to the crystal sizes obtained from XRD analysis. The comparison of our results with previous studies revealed similarities in crystal sizes, diffraction values, and peak points.

3.3. Antimicrobial activity of silver nanoparticles

The antimicrobial effects of AgNPs synthesized through green synthesis from cornelian cherry at two different extraction temperatures were investigated using the paper disk method against *Staphylococcus aureus*, *Listeria monocytogenes*, *Salmonella* Typhi, and *Escherichia coli* O157:H7. The concentrations of bacterial cultures used for determining the antimicrobial activity were found to be $9.9x10^8$ CFU/mL for *Staphylococcus aureus*, $3.8x10^8$ CFU/mL for *Listeria monocytogenes*, $5.7x10^8$ CFU/mL for *Salmonella* Typhi, and $6.7x10^8$ CFU/mL for *Escherichia coli* O157:H7.

The results of the antimicrobial activity of AgNPs synthesized from cornelian cherry extracts obtained at 20 °C and 60 °C are presented in Table 1.

Table 1- Antimicrobial activity of AgNPs synthesized from. cornelian cherry

Microorganism	*AgNP (mg/mL)*	*Cornelian cherry (20 °C) (mm)*			*Cornelian cherry (60 °C) (mm)*		
		CA	*E*	*NP*	*CA*	*E*	*NP*
Staphylococcus aureus	10	30	8	9	27	9	9
	25	28	9	9	30	7	9
Listeria monocytogenes	10	21	7	ND	19	ND	ND
	25	20	9	9	20	8	8
***Salmonella* Typhi**	10	24	7	ND	21	ND	ND
	25	22	8	7	22	7	ND
***Escherichia coli* O157:H7**	10	25	8	9	25	ND	7
	25	22	* ND	ND	21	ND	ND

*ND: not detected CA: Chloramphenicol (30µg), E: Extract, NP: Silver nanoparticle

The positive control, chloramphenicol antibiotic disks, created inhibition zones ranging from 19-30 mm in the Petri dishes. The negative control, cornelian cherry extract, exhibited inhibition zone diameters ranging from 7-9 mm against the tested pathogenic bacteria.

As shown in Table 1, AgNPs synthesized from extracts obtained at 20 °C formed a 9 mm inhibition zone against *Staphylococcus aureus* and *Escherichia coli* O157:H7 cultures at a concentration of 10 mg/mL. However, they did not show any significant activity against the other microorganisms (P>0.05). AgNPs prepared at a 25 mg/mL concentration also formed 9 mm inhibition zones against *Staphylococcus aureus* and *Listeria monocytogenes* cultures and a 7 mm inhibition zone against *Salmonella* Typhi culture (P>0.05). However, they did not exhibit antimicrobial activity against *Escherichia coli* O157:H7 (Figure 18).

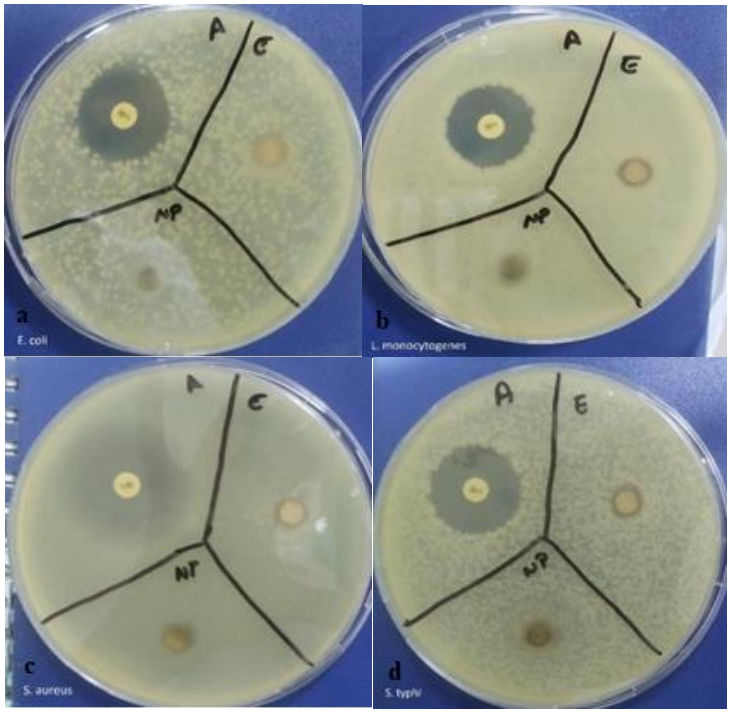

Figure 18- The antimicrobial results of AgNPs synthesized from cornelian cherry extract at 20 °C (25 mg/mL) as follows: (a) *E. coli* O157:H7, (b*) L. monocytogenes*, (c) *S. aureus*, (d) *S.* Typhi.

The antimicrobial activity of AgNPs synthesized from the extract at a temperature of 60 °C and prepared at a concentration of 10 mg/mL, as indicated in Table 1, resulting in the formation of a 9-mm-inhibition zone in *Staphylococcus aureus* culture and a 7-mm-inhibition zone in *Escherichia coli* O157:H7 cultures. However, the AgNPs at a 25 mg/mL concentration exhibited a 9 mm inhibition zone in the *Staphylococcus aureus* culture and an 8 mm inhibition zone in the *Listeria monocytogenes* culture. Notably, both concentrations of AgNPs showed no significant efficacy against *Salmonella* Typhi culture (P>0.05) (see Figure 19).

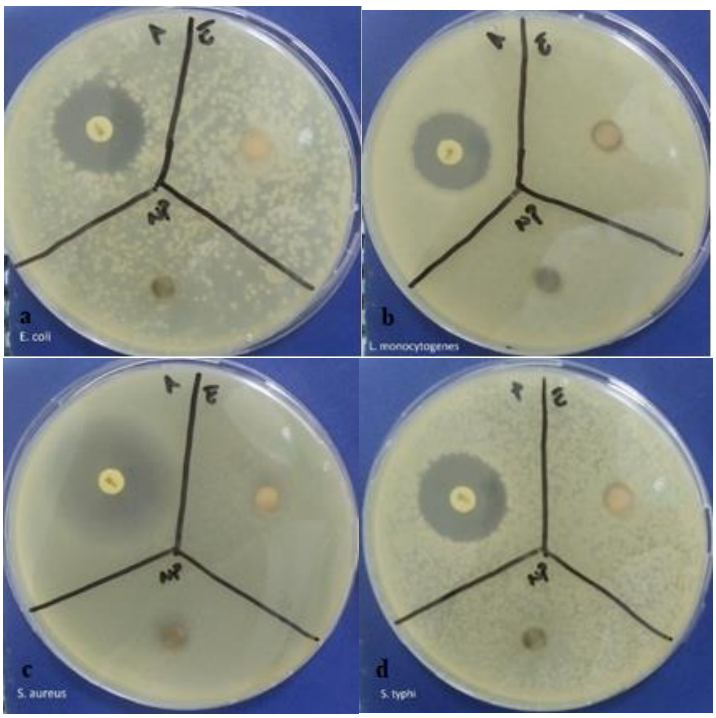

Figure 19- The antimicrobial results of AgNPs synthesized from cornelian cherry extract at 60 °C (25 mg/mL) as follows: (a) *E. coli* O157:H7, (b*) L. monocytogenes*, (c) *S. aureus*, (d) S. Typhi

The studies conducted have demonstrated the antimicrobial effects of AgNPs at various concentrations against certain bacteria. While antimicrobial effects have been observed in studies involving bacteria such as *Escherichia coli*, *Vibrio cholera*, *Bacillus subtilis*, *Bacillus vallismortis*, *Klebsiella pneumoniae*, *Proteus vulgaris*, *Staphylococcus aureus*, and *Aeromonas hydrophila* (Vignesh et al. 2013; Saravanakumar et al. 2017; Kumar et al. 2017b; Pirtarighat et al. 2019; Tailor et al. 2020;), Taghavizadeh Yazdi et al. (2019) reported no antibacterial effect on *Staphylococcus aureus,* and *Bacillus subtilis* at the concentration they utilized.

The results obtained in this study indicate that silver nanoparticles synthesized from cornelian cherry did not exhibit statistically significant activity against pathogenic bacteria ($P>0.05$). It is suggested that the concentrations of 10 and 25 mg/mL used in the experiments may not have been sufficient, and therefore, higher concentrations should be considered in future research.

4. Conclusions

This study presents an innovative approach to nanoparticle synthesis using the environmentally friendly, low-cost, and simple method of utilizing cornelian cherry (*Cornus mas* L.) fruit with high polyphenol content for green synthesis. The observed color change during the formation of nanoparticles, the stable structure of the resulting nanoparticles, their spherical shape, and the silver content over 80% demonstrate the suitability of cornelian cherry, which is known for its high phenolic content, for this purpose. The microbiological study indicates the antimicrobial potential of the resulting nanoparticles and the need for further studies using plants known for their high phenolic content. The increasing resistance of bacteria worldwide to various agents leads to the search for new methods for controlling these bacteria, and studies conducted in this regard demonstrate the usability of AgNPs obtained through green synthesis.

In our research, we have observed that silver nanoparticles offer several advantages for synthesis, including ease of processing, measurability, and economic accessibility. Additionally, Cornelian cherry (Cornus mas L.) demonstrates the capability to form stable nanoparticles that can be stored for extended periods without molecular aggregation. Some studies have investigated the regulation of such nanoparticles through testing, whereas limited attention has been given to plant-based mechanisms. Subsequently, in our studies, it is imperative to identify the key components of *Cornus mas* L. extract and elucidate their roles in the production of AgNPs (silver nanoparticles). Numerous mechanisms have been proposed to account for the antibacterial activity of AgNPs. These mechanisms encompass the release of silver ions from AgNPs, the generation of reactive oxygen species, disruption of cellular morphology, inactivation of crucial enzymes, DNA condensation, and interference with DNA replication. Nevertheless, there is potential for further exploration to develop novel AgNP formulations. Furthermore, comprehensive research should be undertaken to assess the migration of silver ions into food products, and it is essential to establish migration limits to safeguard consumer health.

Acknowledgements

This study was supported by the Manisa Celal Bayar University Research Projects Management Unit (Project No. 2021-033).

References

Abbasi E, Milani M, Fekri Aval S, Kouhi M, Akbarzadeh A, Tayefi Nasrabadi H, Nikasa P, Joo S.W Hanifehpour Y & Nejati-Koshki K (2016). "Silver nanoparticles: synthesis methods, bio-applications and properties". *Critical reviews in microbiology* 42: 173-180. https://doi.org/10.3109/1040841x.2014.912200

Ali Z A, Yahya R, Sekaran S D & Puteh R (2016). "Green synthesis of silver nanoparticles using apple extract and its antibacterial properties". *Advances in Materials Science and Engineering* pp. 1-6. https://doi.org/10.21275/sr231021141519

Alkhattaf F S (2021). "Gold and silver nanoparticles: Green synthesis, microbes, mechanism, factors, plant disease management and environmental risks" *Saudi Journal of Biological Sciences* 28(6): 3624-3631

Alkhalaf M I, Hussein R H & Hamza A (2020). "Green synthesis of silver nanoparticles by *Nigellasativa* extract alleviates diabetic neuropathy through anti-inflammatory and antioxidanteffects". *Saudi Journal of Biological Sciences* 27(9): 2410-2419. https://doi.org/10.1016/j.sjbs.2020.05.005

Ameen F, Srinivasan P, Selvankumar T, Kamala-Kannan S, Al Nadhari S, Almansob A, Dawoud T & Govarthanan M (2019). "Phytosynthesis of silver nanoparticles using *Mangifera indica* flower extract as bioreductant and their broad-spectrum antibacterial activity"" *Bioorganic Chemistry* 88: 102970

Arshadi E, Sedaghat S & Moradi O (2018). "Green synthesis and characterization of silver nanoparticles using fructose". *Asian Journal of Green Chemistry* 2(1): 41-50

Arya A, Mishra V & Chundawat T S (2019). "Green synthesis of silver nanoparticles from green algae (*Botryococcus braunii*) and its catalytic behavior for the synthesis of benzi.midazoles". *Chemical Data Collections* 20: 100190

Baran M F, Umaz A & Eren A (2020). "Antimicrobial applications of silver nanoparticles synthesized from plant origin against some microorganisms" *Fen Bilimleri ve Matematik Alanında Araştırma ve Derlemeler* 93-100. (In Turkish)

Baysal G (2020). "The use of nanosystems in the food industry" *The Journal of Food* 45(3): 517-529. (In Turkish)

Behravan M, Panahi A H, Naghizadeh A, Ziaee M, Mahdavi R & Mirzapour A (2019). "Facile green synthesis of silver nanoparticles using *Berberis vulgaris* leaf and root aqueous extract and its antibacterial activity" *International journal of biological macromolecules* 124: 148-154. https://doi.org/10.1016/j.ijbiomac.2018.11.101

Cao Y, Jin R & Mirkin C A (2001). "DNA-Modified Core− Shell Ag/Au Nanoparticles". *Journal of the American Chemical Society* 123: 7961-7962

Celep E, Aydın A & Yeşilada E (2012). "A comparative study on the in vitro antioxidant potentials of three edible fruits: Cornelian cherry, Japanese persimmon and cherry laurel" *Food and Chemical Toxicology* 50(9): 3329-3335). https://doi.org/10.1016/j.fct.2012.06.010

Ceylan R, Demirbas A, Ocsoy İ, & Aktumsek A (2021). "Green synthesis of silver nanoparticles using aqueous extracts of three *Sideritis* species from Turkey and evaluations bioactivity potentials". *Sustainable Chemistry and Pharmacy* 21: 100426

David L, Moldovan B, Baldea I, Olteanu D, Bolfa P, Clichici S & Filip G A (2020). "Modulatory effects of *Cornus sanguinea* L. mediated green synthesized silver nanoparticles on oxidative stress, COX-2/NOS2 and NFkB/pNFkB expressions in experimental inflammation in Wistar rats". *Materials Science and Engineering: C*, 110: 110709. https://doi.org/10.1016/j.msec.2020.110709

Diler D & Leblebicier Y (2020). "Muşmula (*Mespilus germanica* L.) Silver nanoparticle (AgNP) synthesis and characterization studies in medlar (*Mespilus germanica* L.) extract biocatalyst". *Bilim Armonisi*, 3(1): 17-23. https://doi.org/10.37215/bilar.595127 (In Turkish)

Du J, Hu Z, Yu Z, Li H, Pan J, Zhao D & Bai Y (2019). "Antibacterial activity of a novel *Forsythia suspensa* fruit mediated green silver nanoparticles against food-borne pathogens and mechanisms investigation". *Materials Science and Engineering: C*, 102: 247-253. https://doi.org/10.1016/j.msec.2019.04.031

Ekrikaya S, Yilmaz E, Celik C, Demirbuga S, Ildiz N, Demirbas A & Ocsoy İ (2021). "Investigation of ellagic acid rich-berry extracts directed silver nanoparticles synthesis and their antimicrobial properties with potential mechanisms towards *Enterococcus faecalis* and *Candida albicans"*. *Journal of Biotechnology* 341: 155–162

Filip G A, Moldovan B, Baldea I, Olteanu D, Suharoschi R, Decea N, Cismaru C M, Gal E, Cenariu M, Clichici S & David L (2019). "UV-light mediated green synthesis of silver and gold nanoparticles using cornelian cherry fruit extract and their comparative effects in experimental inflammation". *Journal of Photochemistry and Photobiology B: Biology* 191: 26-37. https://doi.org/10.1016/j.jphotobiol.2018.12.006

Ghaedi M, Yousefinejad M, Safarpoor M, Khafri H Z & Purkait M K (2015). "*Rosmarinus officinalis* leaf extract mediated green synthesis of silver nanoparticles and investigation of its antimicrobial properties". *Journal of Industrial and Engineering Chemistry* 31: 167-172. https://doi.org/10.1016/j.jiec.2015.06.020

Gulbagca F, Ozdemir S, Gulcan M & Sen F (2019). "Synthesis and characterization of *Rosa canina*-mediated biogenic silver nanoparticles for anti-oxidant, antibacterial, antifungal, and DNA cleavage activities". *Heliyon* 5(12): e02980

Hashim N, Paramasivam M, Tan J S, Kernain D, Hussin M H, Brosse N, Gambier F & Raja P B (2020). "Green mode synthesis of silver nanoparticles using *Vitis vinifera*'s tannin and screening its antimicrobial activity/apoptotic potential versus cancer cells". *Materials Today Communications* 25: 101511. https://doi.org/10.1016/j.mtcomm.2020.1 01511

He Y, Li X, Wang J, Yang Q, Yao B, Zhao Y, Zhao A, Sun W & Zhang Q (2017). "Synthesis, characterization and evaluation cytotoxic activity of silver nanoparticles synthesized by Chinese herbal *Cornus officinalis* via environment friendly approach". *Environmental Toxicology and Pharmacology* 56: 56-60

Hernandez-Morales L, Espinoza-Gómez H, Flores-López L Z, SoteloBarrera E L, Núñez-Rivera A, Cadena-Nava R D, Alonso- Núñez G & Espinoza K A (2019). "Study of the green synthesis of silver nanoparticles using a natural extract of dark or white *Salvia hispanica L*. seeds and their antibacterial application". *Applied Surface Science* 489: 952-961. https://doi.org/10.1016/j.apsusc.2019.06.031

Hernandez-Pinero J L, Terrón-Rebolledo M, Foroughbakhch R, Moreno-Limón S, Melendrez M F, Solís-Pomar F & Pérez-Tijerina E (2016). "Effect of heating rate and plant species on the size and uniformity of silver nanoparticles synthesized using aromatic plant extracts". *Applied Nanoscience* 6(8): 1183-1190

KaviyaS, Santhanalakshmi J, Viswanathan B, Muthumary J & Srinivasan K (2011). "Biosynthesis of silver nanoparticles using *Citrus sinensis* peel extract and its antibacterial activity". *Spectrochimica Acta Part A: Molecular and Biomolecular Spectroscopy* 79(3): 594-598. https://doi.org/10.1016/j.saa.2011.03.040

Korkmaz N, Ceylan Y, Hamid A, Karadağ A, Bülbül A S, Aftab M N, Çevik Ö & Şen F (2020). "Biogenic silver nanoparticles synthesized via *Mimusops elengi* fruit extract, a study on antibiofilm, antibacterial, and anticancer activities". *Journal of Drug Delivery Science and Technology* 59: 101864. https://doi.org/10.1016/j.jddst.2020.101864

Kumar B, Smita K, Cumbal L & Debut A (2017a). "Green synthesis of silver nanoparticles using Andean blackberry fruit extract". *Saudi journal of biological sciences* 24(1): 45-50. https://doi.org/10.1016/j.sjbs.2015.09.006

Kumar R, Ghoshal G, Jain A & Goyal M (2017b). "Rapid green synthesis of silver nanoparticles (AgNPs) using (*Prunus persica*) plants extract: exploring its antimicrobial and catalytic activities". *J. Nanomed. Nanotechnol*, *8*(4): 1-8

Lopes C R B & Courrol L C (2018). "Green synthesisof silver nanoparticles with extract of *Mimusopscoriacea* and light". *Journal of Luminescence*, 199: 183-187

Paiva-Santos A C, Herdade A M, Guerra C, Peixoto D, Pereira-Silva M, Zeinali M, Mascarenhas-Melo F, Paranhos A & Veiga F (2021). "Plant-mediated green synthesis of metal-based nanoparticles for dermopharmaceutical and cosmetic applications". *International Journal of Pharmaceutics* 597: 120311

Pallela P N V K, Ummey S, Ruddaraju L K, Pammi S V N & Yoon S G (2018). "Ultra Small, monodispersed green synthesized silver nanoparticlesusing aqueous extract of *Sida cordifolia* plant andinvestigation of antibacterial activity". *Microbial Pathogenesis* 124: 63-69. https://doi.org/10.1016/j.micpath.2018.08.026

Pirtarighat S, Ghannadnia M & Baghshahi S (2019). "Green synthesis of silver nanoparticles using the plant extract of *Salvia spinosa* grown in vitro and their antibacterial activity assessment". *Journal of Nanostructure in Chemistry* 9(1): 1-9

Polat S & Fenercioğlu H (2014). "Nanotechnology applications in food packaging: Use of inorganic nanoparticles". *Gıda* 39(3): 187-194. (In Turkish)

Rai V R & Bai J (2011). "Nanoparticles and their potential application as antimicrobials". Ed.: A. Méndez-Vilas, Microbiology Series No. 3 Vol. 1, Spain pp. 197-209

Ramkumar V S, Pugazhendhi A, Gopalakrishnan K, Sivagurunathan P, Saratale G D, Dung T & Kannapiran E (2017). "Biofabricationand characterization of silver nanoparticles usingaqueous extract of seaweed *Enteromorphacompressa* and its biomedical properties". *Biotechnology Reports* 14: 1-7

Rana A, Yadav K & Jagadevan S (2020). "A comprehensive review on green synthesis of nature-inspired metal nanoparticles: mechanism, application and toxicity". *Journal of Cleaner Production* 272: 1-25. https://doi.org/10.1016/j.jclepro.2020.122880

Rezvani E, Rafferty A, McGuinness C & Kennedy J (2019). "Adverse effects of nanosilver on human health and the environment". *Acta Biomaterialia* 94: 145-159

Salejda A M, Kucharska A Z & Krasnowska G (2018). "Effect of cornelian cherry (*Cornus mas* L.) juice on selected quality properties of beef burgers". *Journal of Food Quality*, Article ID 1563651. https://doi.org/10.1155/2018/156365

Saravanakumar A, Peng M M, Ganesh M, Jayaprakash J, Mohankumar M & Jang H T (2017). "Low-cost and eco-friendly green synthesis of silver nanoparticles using *Prunus japonica* (Rosaceae) leaf extract and their antibacterial, antioxidant properties". *Artificial Cells, Nanomedicine, and Biotechnology* 45(6): 1165-1171

Silver S (2003). "Bacterial silver resistance: Moleculer biology and uses and misuses of silver compounds". *FEMS Microbiology Reviews* 27(2-3): 341-353

Stankovic M S, Zia-Ul-Haq M, Bojovic B M & Topuzovic M D (2014). "Total phenolics, flavonoid content and antioxidant power of leaf, flower and fruits from cornelian cherry (*Cornus mas* L.)". *Bulgarian Journal of Agricultural Science* 20(2): 358-363.

Sürengil G & Kılınç B (2011). "Gıda ambalaj sektöründe nanoteknolojik uygulamalar ve su ürünleri açısından önemi". *Journal of Fisheries Sciences* 5(4): 317-325

Taghavizadeh Yazdi M E, Modarres M, Amiri M S & Darroudi M (2019). "Phyto-synthesis of silver nanoparticles using aerial extract of *Salvia leriifolia* Benth and evaluation of their antibacterial and photo-catalytic properties". *Research on Chemical Intermediates* 45(3): 1105-1116. https://doi.org/10.1007/s11164-018-3666-8

Tailor G, Yadav B L, Chaudhary J, Joshi M & Suvalka C (2020). "Green synthesis of silver nanoparticles using *Ocimum canum* and their anti-bacterial activity". *Biochemistry and Biophysics Reports* 24: 100848. https://doi.org/10.1016/j.bbrep.2020.100848

Thomas B, Vithiya B, Prasad T, Mohamed S B, Magdalane C M, Kaviyarasu K & Maaza M (2019). "Antioxidant and photocatalytic activity of aqueous leaf extract mediated green synthesis of silver nanoparticles using *Passiflora edulis f. flavicarpa". Journal of Nanoscience and Nanotechnology* 19(5): 2640-2648

Vignesh, V, Anbarasi K F, Karthikeyeni S, Sathiyanarayanan G, Subramanian P & Thirumurugan R (2013). "A superficial phyto-assisted synthesis of silver nanoparticles and their assessment on hematological and biochemical parameters in *Labeo rohita* (Hamilton, 1822)". *Colloids and Surfaces A: Physicochemical and Engineering Aspects* 439: 184-192. https://doi.org/10.1016/j.colsurfa.2013.04.011

Vijayakumar S, Malaikozhundan B, Saravanakumar K, Durán-Lara E F, Wang M H & Vaseeharan B (2019). "Garlic clove extract assisted silver nanoparticle–Antibacterial, antibiofilm, antihelminthic, anti-inflammatory, anticancer and ecotoxicity assessment". *Journal of Photochemistry and Photobiology B: Biology* 198: 111558

Wang S, Lawson R, Ray P C & Yu H (2011). "Toxic effects of gold nanoparticles on *Salmonella* Typhimurium bacteria". *Toxicology and Industrial Health* 27(6): 547-554